

Braking energy recuperation for electric traction drive in urban rail transit network based on control super-capacitor energy storage system

Braking energy in Electric traction system of electric trains is significant because of trains' frequent accelerating, braking process, so braking energy recovery of urban rail vehicles has been one of the primary objectives in recent years. Energy saving technologies in the railway electric traction field can be mainly divided into two domains: The first one enhances efficiency of traction equipment, such as power electronics converters or traction motors. The other is recovery of kinetic energy in deceleration process of electrified train by applying energy storage devices, or active rectifiers, reversible rectifiers placed to traction substations. The paper presents a regenerative braking energy recovery system based on super-capacitor energy storage system. When electric trains operate in accelerating or braking regimes, the voltage of DC bus will fluctuate sharply to compare with its normal voltage level; therefore, an energy charge /discharge system should be used to not only manage the power flow but also adjust the voltage of the metro contact electric network. For these reasons, super-capacitor energy storage system (SESS) will be integrated to traction motor drive system to recuperate regenerative braking energy in braking phase and support energy for acceleration phase. Braking energy will be stored in the super capacitors thanks to a bidirectional DC-DC converter interface, and designing control strategy for energy exchange between line utility with traction drive system is to manage UDC-link at a fixed value. At the end, simulation results of the whole system which includes power supply unit, traction motor, driven controller, super-capacitors, Interleaved bidirectional DC-DC converter of line 2 Cat Linh-Ha Dong, Viet Nam have been verified on Matlabsimulink, Simpower system.

Keywords: Bidirectional DC-DC converter, super-capacitor energy storage system (SESS), traction motor drive

Article history: Received 24 January 2017, Accepted 11 August 2018

1. Introduction

Nowadays, urban railway transit has attracted more and more attentions because they prove to be a more efficient and less emissive transportation system, reducing traffic jam compared to other means of transportation. Statistic data show that braking energy absorbed by adjacent trains is about 20% - 30%, and the rest one primarily consumed by braking resistance, which leads to both massive energy waste and temperature increment into the environment [1,2,3]. In Vietnam, The construction of urban railway transit systems in Ha Noi and Ho Chi Minh cities is getting underway; therefore, saving energy in urban railway being a hot issue needs to be done research. there are some saving energy solutions including: timetable optimization, slope distance optimization, power management optimization, running resistance reduction, maximum traction force, maximum braking force increase, regenerative braking energy recovery, reduction of traction motor, converter

* Corresponding author: Phuong Vu, PhD, School of Electrical Engineering, Hanoi University of Science and Technology, Hanoi, Vietnam

Email: phuong.vuhoang@hust.edu.vn

¹ University of Transport and Communications, Hanoi, Vietnam

² School of Electrical Engineering, Hanoi University of Science and Technology, Hanoi, Vietnam

losses[4,5,6], among these studies, the article has focused onbraking energy recuperation of electrified trains because of high energy-saving %, quality stability of power supply system, as well [5]. Fig. 1, 2 show the typical DC transit system and vehicle traction motor characteristic[7].

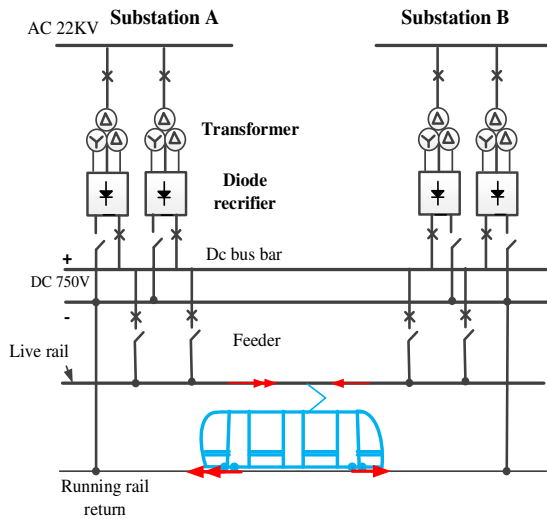


Figure 1. Two side supplied DC line

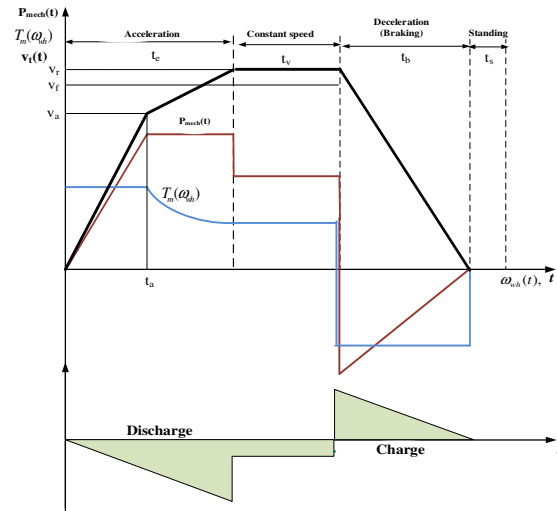


Figure 2. Operating characteristics of traction motor drive system integratedwith SESS

In Viet Nam, the DC traction system is also going to operate at two kinds of voltage levels in the metro contact network:750V, 1500V DCbased on rectifier substations, generally connected to medium-voltage distribution networks22kVAC. Fig. 1 showsthe metro network model includes electrified train, unidirectional substations, connecting lines, and fig. 2 demonstrates the performance characteristics of metro train [7]. As well known, the typical driving cycle of railway vehicle comprises of five regimes:powering, cruising, coasting, braking, standing phases. If distances between stations are short, the driving cycle will have four different motion states of operation: acceleration, constant speed, braking (decelerating) and standstill. During powering, the vehicle absorbs energy from the feeder line, causing the voltage drop, whilebraking, the vehicle turns back energy to the feeder, leading to the vehicle pantograph voltage to rise beyond the allowable value [8,9,10,11,12,13,14,15,16,17].Therefore, it is very important to conduct research on improving the energy efficiency and reliable, safe operation in electrical railway systems. In this paper, the authors have proposed traction drive system integrated with super-capacitor energy storage because of fast charge/discharge time of super-capacitor banks being suitable for frequent acceleration/deceleration of urban electric trains [18,19,20,21] and designedcontrol strategy for the energy storage system by controlling UDC-link at fixed value to ensure energy exchange between line source and load in suppressing voltage fluctuation, preventing the failure of regenerative braking, and saving energy consumption of vehicle operation[22,23]. Simulation results on Matlab Simulink/Simpower system have verified the feasibility of this strategy.

2. System model of regenerative braking

The 22KV AC supply is transformed and rectified to provide the correct 750V DC traction voltage. A three-phase diode bridge rectifier is modelled as the substation rectifier in actual system and supplies power at 750V DC , and this type of substation only allows power flows from the utility network to the railway system. Inside train, the main circuit of the AC motor driven vehicle includes: a three phase voltage source inverter (VSI) is driving induction motor (IM), the traction load system is derived from mechanical dynamics of the train-wheel-track interactive system. When the voltage of DC bus is higher, the super-capacitor energy storage system absorbs the excess energy in super-capacitors by bidirectional DC-DC converter interface to recover regenerative energy instead of energy dissipation by braking resistors. When the voltage of DC bus is lower, SESS will discharge to support the network voltage level instead of relying on traction substations.

The whole traction system integrated with super-capacitor storage system for urban railway transportation contains these main components (as shown in fig.3): power supply, traction motor, voltage source inverter, super-capacitor bank and interleaved bidirectional DC/DC converter, braking chopper.

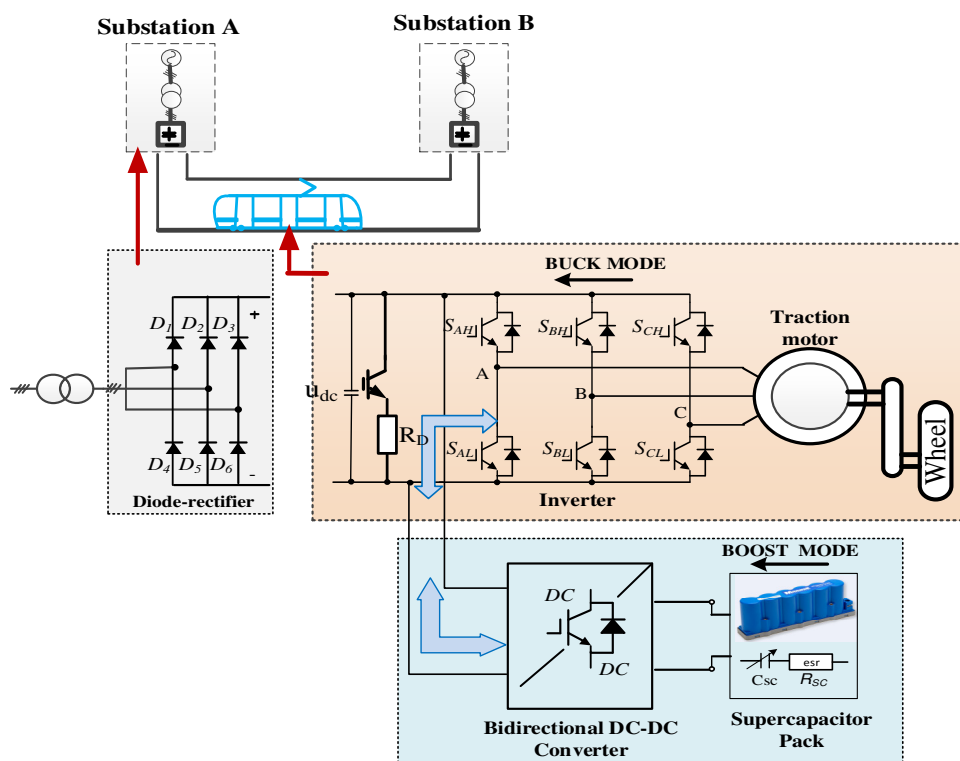


Figure 3. Configuration of traction motor with SCES

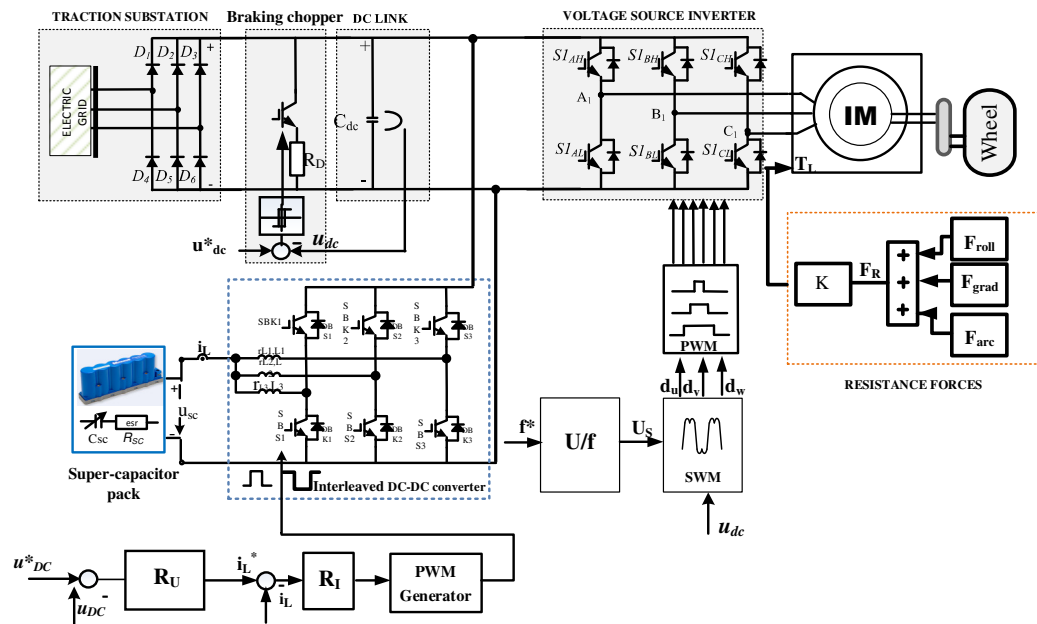


Figure 4. Block diagram of control traction motor drive system integrated with SESS

The structure of the system control is deduced from the block diagram depicted in Fig.4. Three parts are considered: The resistance forces against train motion, voltage source inverter fed traction motor drive with control -variable-voltage variable-frequency (VVVF), and energy recovery control by control design of interleaved bidirectional DC-DC converter in order to recuperate regenerative braking energy by supercapacitor energy storage device in braking mode; furthermore, to manage the energy balance between line utility and traction load.

2.1 Dynamic model of electric train

In the study, it has been concentrated on an electric train having four bogies (T-M-T-M), two wheelsets in each bogie, eight traction motors placed on two bogies, and each motor is mounted on each corresponding wheelset by a gearbox, respectively. Important variables standing for railway vehicle dynamics are position, speed and acceleration. During the train movement, relations among these variables are computed according to Newton's second law of motion as following [24,25]:

$$M_{mass} a = F_{tr} - F_R \quad (1)$$

Where,

- M_{mass} Total effective mass of train
- F_{tr} Traction force
- F_R Total resistance force
- a Acceleration of the train

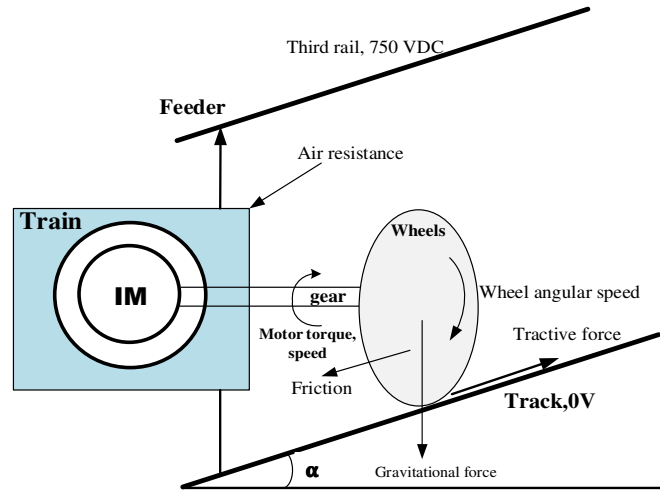


Figure 5. Torques and forces act on the rail wheel

Fig 5 shows forces acting on the train in which the total resistance force comprising of the air resistance F_{aero} , the rolling resistance F_{roll} , the gravitational force F_{grad} , the arc resistance F_{arc} is represented in equation (2)

$$\begin{cases} F_R = F_{roll} + F_{aero} + F_{grad} + F_{crv} \\ F_{roll} + F_{aero} = A + Bv + Cv^2 \\ F_{grad} = Mg \sin \alpha \\ F_{arc} = \frac{700}{R} \end{cases} \quad (2)$$

The constants A, B, C are available from the train manufacturer

- g The gravity acceleration
- α The rail path slope
- R Arc radius of rail path

The train and wheel dynamics is given by [26] :

$$T_{el} - T_L = J \frac{d\omega_r}{dt}; \quad J = J_m + J_{eq} \quad (3)$$

Where,

- T_{el} Electromagnetic torque
- T_L Load torque of the IM
- J_m Inertia of the IM
- J_{eq} Equivalent train inertia referred to the IM shaft

The equivalent inertia referred to the one machine shaft is computed:

$$J_{eq} = \frac{1}{4} \frac{M_{mas}}{N} \left(\frac{D_{wh}}{\tau} \right)^2 \quad (4)$$

Where,

- D_{wh} Wheel diameter
- N Number of motors

τ Transmission ratio

The load torque T_L is calculated by[27]

$$T_L = \frac{F_R D_{Wh}}{2\tau\eta_{em}\eta_{mech}} = KF_R \tag{5}$$

Given,

$$K = \frac{D_{Wh}}{2\tau\eta_{em}\eta_{mech}}$$

η_{em} Rated electrical motorefficiency

η_{mech} Rated gear box efficiency

2.2 Model of interleaved bidirectional DC-DC converter

Energy storage system comprises of super-capacitor energy storage device and an interleaved bidirectional DC-DC converter which is considered the interface exchanging energy between traction motor drive with high voltage and super-capacitors with low voltage[28,29,30,31,32].The controller for the interleaved bidirectional DC-DC converter is designed to control $U_{DC-link}$ at fixed value in order to balance energy of line source and load.Power circuit diagram of the three-phase interleaved bidirectional DC-DC converter depicted in Fig.6is able tottransfer energy from SESS to electric drive system, and vice versa.

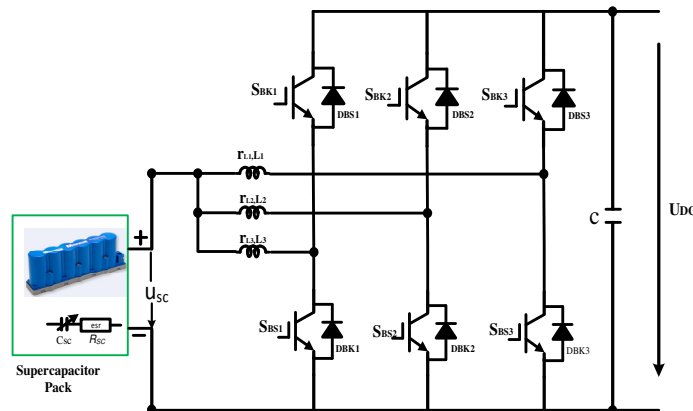


Figure 6.Power electric scheme of a three phase Interleaved DC-DC converter

The main structure of the bidirectional non-isolated DC-DC converter shown in Fig.6contains an inductor, switches S_{BK} and S_{BS} , and diodes are connected in parallel and then to a single capacitor. The DC-DC converter placed between high voltage DC bus and low voltage SESS operates in buck or boost mode: In boost mode, S_{BS} and D_{BS} are the operating switches, and the low-voltage side delivers energy to the high-voltage side (DC bus); super-capacitor modules get discharged by low voltage. In buck mode, S_{BK} and D_{BK} are the operating switches, and the high voltage side transfers energy to the low voltage side; the super-capacitor modules get charged from the DC bus.

Averaged model of bidirectional DC-DC converter is shown in fig.6, switches are replaced by an ideal transformer with $d(t)$ being transformer factor, and

$$\begin{cases} u_1(t) = d(t)u_2(t) \\ i_2(t) = d(t)i_1(t) \end{cases} \tag{6}$$

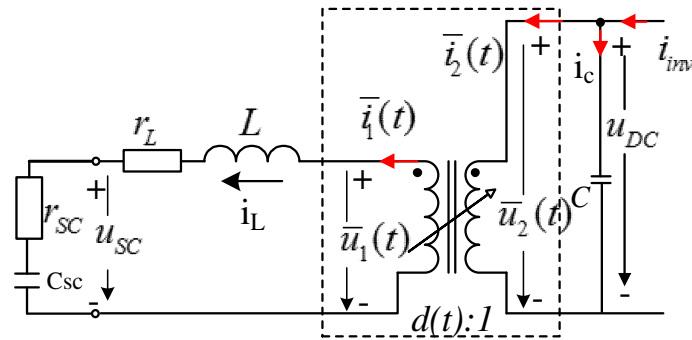


Figure 7. Equivalent circuit of averaged model of bidirectional DC-DC converter

Averaged model of DC-DC bidirectional converter shown average model is[33]

$$\begin{cases} L \frac{di_L}{dt} = -r_L i_L + du_{DC} - u_{sc} \\ C \frac{du_{DC}}{dt} = -di_L + i_{inv} \end{cases} \quad (7)$$

In the equation (7), the state variables are i_L, u_{DC} and control variable is duty ratio (d). The system is nonlinear structure due to existing the multiplication of d and u_{DC} . There are many methods of nonlinear control design; however, in this paper the authors used Linearization around the selected operating point.

3. Control design for interleaved bidirectional DC-DC converter

The cascaded control strategy should be designed to meet the current and voltage requirements [32]. In this study, the PI controllers are designed to keep DC-link voltage at a certain constant value regardless of the variations of load and input voltage. Fig. 8 shows the diagram of the dual-loop control structure in the s-domain.

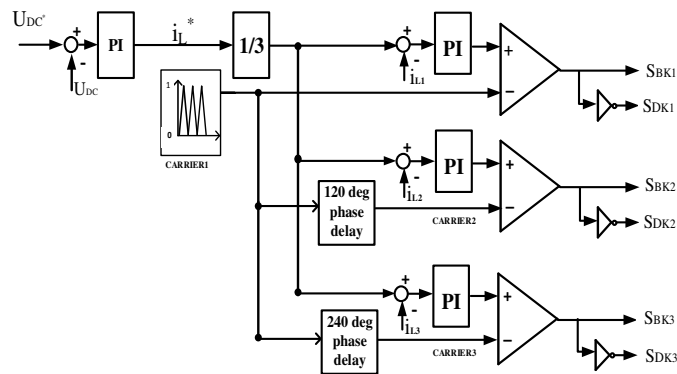


Figure 8. Cascaded loop control structure of the bidirectional DC-DC converter

The outer loop is the voltage loop regulating error between u_{DC} and u_{DC}^* , which generates the current reference for the inner current loop. This control structure requires the sampling of two variables, u_{DC} and i_L . The inner plant captures the inductor current dynamics; namely, managing charge or discharge of super-capacitor system (SC) while the outer plant embeds the equivalent capacitor voltage dynamics.

3.1. Design of the PI current-loop control algorithm

The two-loop control structure requires separation of the dynamics in the sense that the inner loop must act 10 times faster than the outer loop. The inner loop controls charge and discharge of SC;

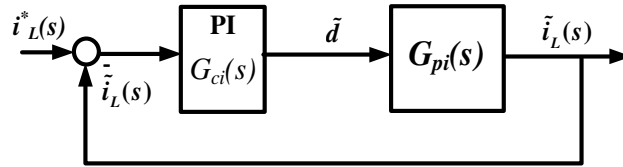


Figure 9. Current-loop control structure

From the first equation of (7), setting

$$L \frac{d\tilde{i}_L}{dt} = -R_L \tilde{i}_L + \tilde{d} U_{DC} - U_{SC} \quad (8)$$

In steady state, u_{SC} may be considered as constant and therefore acts as constant disturbance for the control loop. It can be compensated by feed-forward control.

Therefore, the transfer function relating the inductor current with the voltage $u_{control}$ is computed:

$$G_{pi}(s) = \frac{\tilde{i}_L(s)}{\tilde{d}(s)} = \frac{k}{Ts + 1} \quad (9)$$

The corresponding PI current controller transfer function is given by

$$G_{ci}(s) = k_{pi} \left(1 + \frac{1}{T_i s} \right) = k_{pi} \left(\frac{1 + T_i s}{T_i s} \right) \quad (10)$$

The closed-loop transfer function of fig.7 is shown in (11)

$$G_{Si}(s) = \frac{1 + T_i s}{(T_i T / k_{pi} k) s^2 + T_i [1 + (1 / k_p k)] s + 1} \quad (11)$$

Where T' - the smaller is the better

The best PI controller performance was gained when the plant's dominant pole was cancelled by the controller (10). Thus, the zero at $-\frac{1}{T_i}$ was assigned to the time constant of the plant, which was $T_i = T = \frac{L}{r_L}$, and k_p - the larger is the better.

3.2 Design of the PI voltage-loop control algorithm

After designing current controllers, authors keep designing the voltage-loop control algorithm. For the small perturbations, the current loop acts extremely fast, and it can be assumed ideally with a gain of unity.

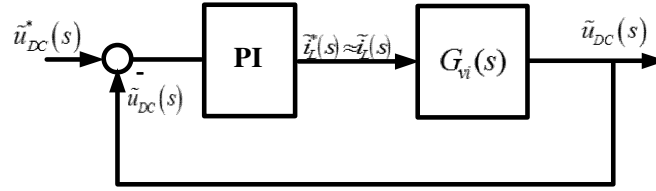


Figure 10.Voltage-loop control structure

Form the second equation of (1) the transfer function relating the voltage u_{DClink} with the inductor current is computed:

$$c \frac{d\tilde{u}_{DC}}{dt} = -(\tilde{d}I_L + \tilde{i}_L D) + \tilde{i}_{inv} \quad (12)$$

Applying the Laplace transform for (13) leads to (14)

$$G_{vi}(s) = \left. \frac{\tilde{u}_{DC}(s)}{\tilde{i}_L(s)} \right|_{\substack{\tilde{d}=0 \\ \tilde{i}_{inv}=0}} \cong \left. \frac{\tilde{u}_{DC}(s)}{\tilde{i}_L^*(s)} \right| = -\frac{D}{Cs} \quad (13)$$

The transfer function of outer plant is type of the integral form. However, the system still exists disturbance, so digital PI controller may be effectively used to ensure both zero steady-state error and controlled bandwidth.

The transfer function of PI

$$G_{vc}(s) = k_{pv} + \frac{k_{Iv}}{s} = \frac{k_{pv}s + k_{Iv}}{s} \quad (14)$$

According to [12], using model balance method finds values of k_{pv}, k_{Iv}

$$G_S(s) = -\frac{(k_{pv}s + k_{Iv})D}{Cs^2 - k_{pv}Ds - k_{Iv}D} \triangleq \frac{k}{\frac{1}{\omega_n^2}s^2 + \frac{2\xi}{\omega_n}s + 1} \quad (15)$$

For our study, the selected values were:

$$\begin{cases} k_{Iv} = -\frac{1}{D} \\ k_{pv} = -\frac{2\xi}{\omega_n D} \\ \omega_n = \frac{1}{\sqrt{C}} \end{cases} \quad (16)$$

Where ω_n - Oscillation cycle, ξ - Damping ratio (select $\xi = 0.71$)

4. Simulation results

Simulation results were performed for the metro-train line 2 Cat linh - Ha dong, Vietnam, 13km in length, including 13 stations, 6 traction substations, 12 trains running up-line and down-line; each train with 4 cars. The behaviour of the metro-train line 2 Cat linh - Ha dong equipped with or /without SESS. The traction train is made of a variable speed drive with induction motors controlled by a variable-voltage variable-frequency (VVVF)

controller by means of V/f technique [34],and simulation parameters for line 2 Cat linh-Ha dong shown in Tab.

Table 1 Parameters of electrical traction motor

Parameters of IM	Unit	Value
Nominal power (P_{nom})	[kW]	160
Nominal speed (n_{nom})	[rpm]	1480
Nominal voltage (U_{nom})	[V]	400
Nominal current (I_{nom})	[A]	290
Stator frequency (f_s)	[Hz]	50
Pole pairs (z_p)	—	2
Rotor resistance (R_r)	[Ω]	0.007728
Stator resistance (R_s)	[Ω]	0.01379
Rotor leakage inductance (σ_r)	[mH]	0.152
Stator leakage inductance(σ_s)	[mH]	0.152
Mutual inductance (L_m)	[mH]	7.69
Inertia (J)	[kgm ²]	2.9
Power factor	$\cos\phi$	0.9

Table 2 Main parameters of the simulated metro train

Parameters of metro train	Unit	Value
Train gand-up	2M2T	
Full load translating mass (M_{mass})	[kg]	247000
Number of electrical traction unit (N)		08
Max speed (v_{max})	[km/h]	80
Base speed (v_b)	[km/h]	35
Max acceleration/braking rates	[m/s ²]	0.94/1
Motion resistance (A)	[KN]	7.75
Motion resistance coefficient (B)	[kg/s]	0.062367
Motion resistance coefficient (C)	[kg/m]	0.00113
Wheel diameter (D_{wh})	[m]	0.84
Transmission ratio (\mathcal{T})		5.3:1
Gear box efficiency (η_{mech})	%	0.95
Motor efficiency (η_{em})	%	0.9
Braking resistor (R_D)	Ω	4
Train inertia (J_{eq})	[kg.m ²]	179

Table 3 Parameters of interleaved bidirectional DC-DC converter

Parameters of DC-DC converter	Symbol	Value
SwitchingFrequency	f_s	5 KHz
DC Link voltage	U_{DC}	750V
Capacitor of DC-Link capacitor	C	7000 μ F
Phase inductance	$L_1 = L_2 = L_3$	2 mH
Phase resistance	r_L	0.05 Ω
Parameters of super-capacitor BMOD0063 P125 B08 63F/125V		

Table 4 Track profile of Metro line 2 Cat linh - Ha dong from Cat linh station to La thanhstation.

Station	Length (m)	Gradient (0/00)	Radius curv. (m)
	87	0,00	0
	206	8,00	0
Cat linh - La thanh	277	0,00	0
(900m)	100	0.00	300
	280	-7,00	400
	50	0,00	0

To verify the controllers and the energy storage performance,cases are studied in this paper with typical two stations: from Cat Linh to La Thanh. Simulation scripts: In the first case, Train 1 is in acceleration, Train 2 is in braking and no energy storage system installed on board; in the second case,both Train 1 and Train 2 are in acceleration without energy storage system;in the third case being similar to the second case, but having the energy storage system.Simulation results are performed with technical parameters of line 2 Cat linh-Ha dong, Viet Nam in tables 1,2,3; gradient at various locations shown in table 4, with running time 68s from Cat Linh station to La Thanh station;interval of 30s after each station; and distance between two stations is 900m; power supply voltage 750VDC; 01 traction motor (It is assumed that the role of 08 traction motors are the same, so simplistically, only 01 traction motor is under consideration).

Case 1: Train 1 is in braking phase at t=48s, train 2 starts accelerating at t=48s, without SESS

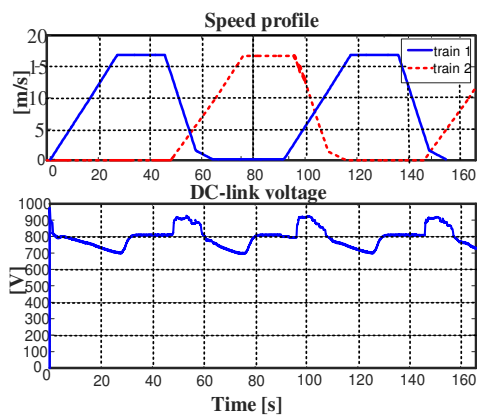


Figure11.Profile of two trains and dynamic behaviors of DC-link voltage

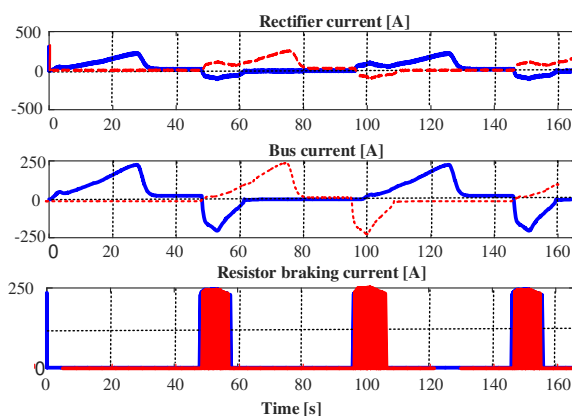


Figure12. Dynamic behaviors of rectifier, bus, resistor braking Currents

Fig 11 shows T1 barks on at t=0s, acceleration phase in 28s(17s, 87m, base speed 35km/h equal to 9.72m/s; 11s, 206m, max speed 60km/h equal to 16.7 m/s); Constant speed phase (20s, 337m, constant speed 16.7 m/s); and braking phase (20s until it stops, 330m) is devised into two braking modes: Regenerative braking mode with train speed \geq 5km/h equal to 1.4m/s, and dynamic braking with train speed $<$ 5km/h to 0km/h, while T1 is in braking phase, T2 starts operating at t=48s. Naturally, T1 and T2 exchanges energy each other; namely, surplus energy of T1 transferred to T2. As a results, voltage of DC-link fluctuates from 900 VDC to 700 VDC in allowed operating voltage level (500 to 900VDC).

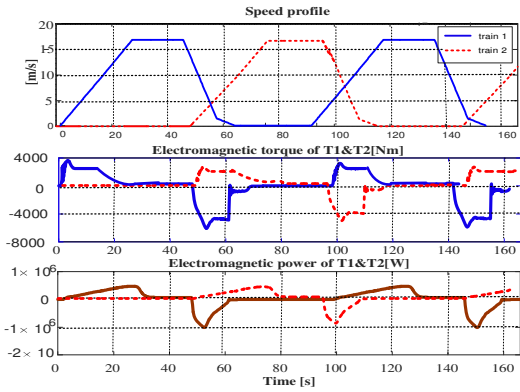


Figure 13. Dynamic behaviors of torque and power

When speed of train from 0 to 35 km/h; electromagnetic torque is unchanged to 2800Nm, speed from 35km/h to 60 km/h electromagnetic torque is weakened; regenerative braking phase of train from 60km/h to 5km/h, electromagnetic torque is negative 5000Nm shown Fig 13. Fig 14 indicated resistance forces: fiction, grad, load torque acting on traction motor simulated by survey parameters from metro line 2 Cat Linh-Ha Dong, Viet Nam.

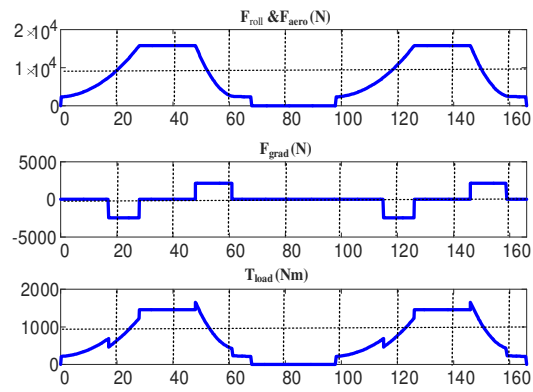


Figure 14. Dynamic behaviors of resistance forces and load torque

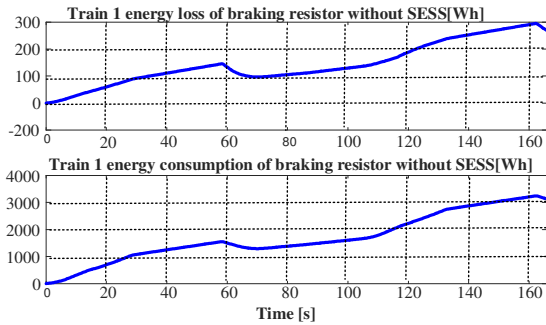


Figure 15. Dynamic behaviors of T1 energy, no SESS

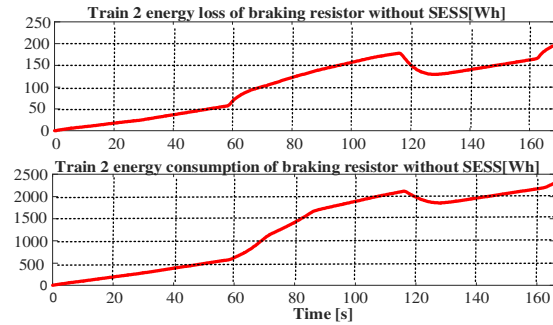


Figure 16. Dynamic behaviors of T2 energy, no SESS

Case 2: Train 1 is in accelerating phase at t=0s, train 2 also starts accelerating at t=0s, without SESS

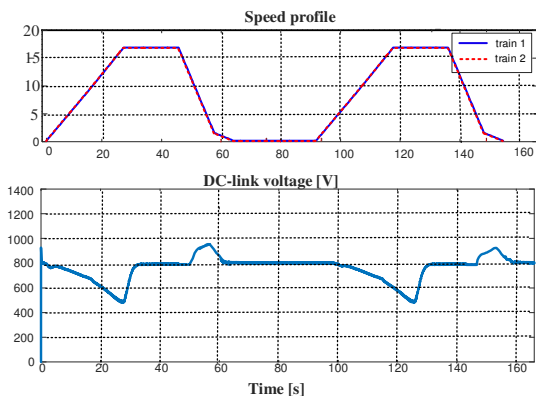


Figure 17. Profile of two trains and dynamic behavior of DC-link voltage

Fig 17 shows the DC-link voltage sharply drops from 860V to 480V, while operating voltage compliant with EN 50163 is allowed from 500 VDC to 900 VDC, braking energy on resistor bank occurs from t=48s to 63s; t=146s to 161s equivalent to resistor braking currents shown fig.18.

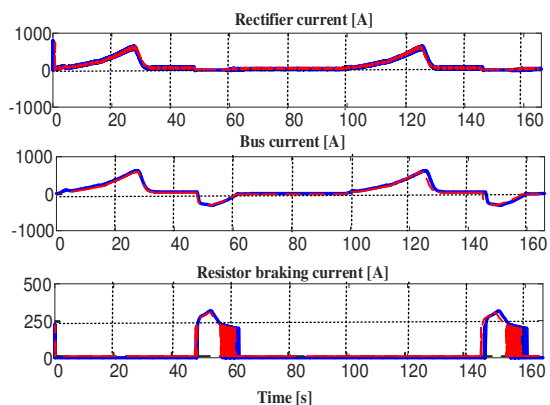


Figure 18. Dynamic behaviors of rectifier, bus, resistor braking currents

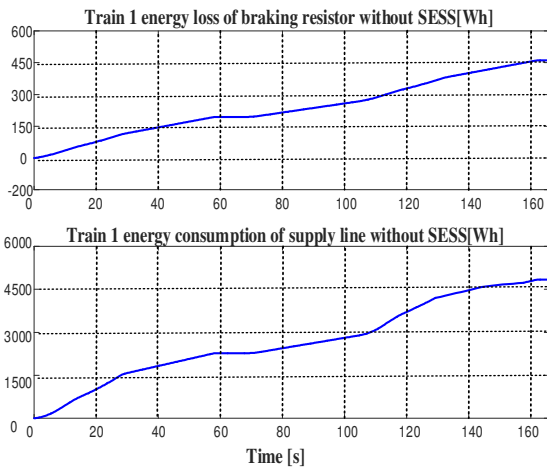


Figure 19. Dynamic behaviors of T1 energy, no SESS

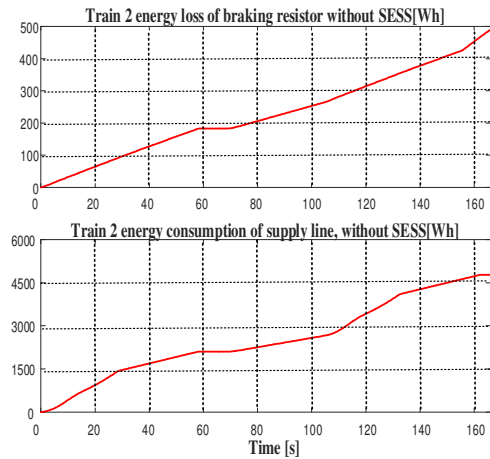


Figure 20. Dynamic behaviors of T2 energy, no SESS

Case 3: Train 1 is in accelerating phase at $t=0s$, train 2 also starts accelerating at $t=0s$, SESS integrated with traction motor drive system.

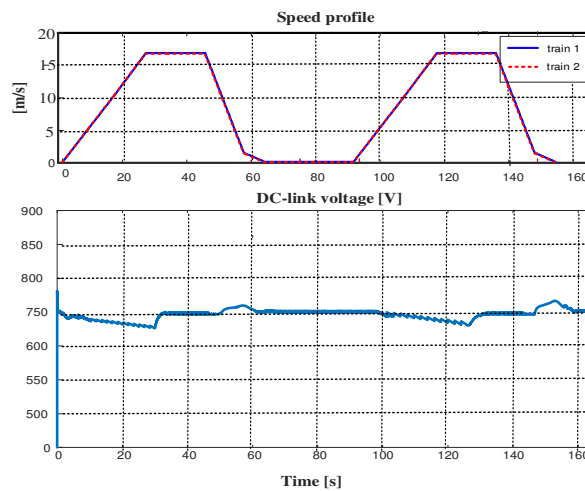


Figure 21. Dynamic behavior of U_{DClink} with SESS

In circumstance, both electric trains accelerate, simulation aims to evaluate the contribution of super-capacitors during acceleration of the vehicle and their regenerative braking energy recovering capability during braking phase.

When traction motor drive is disconnected with SESS, the surge voltage of the line is avoided at timings of changing operation states of train ($t=48s$ to $t=63s$; $t=146s$ to $t=161s$) shown fig.21, and DC-link voltage fluctuates slightly from 730 VDC to 770 VDC around reference voltage value at 750 VDC. The light voltage fluctuation is thanks to SESS. SESS will discharge energy to support train's acceleration phase, and charge surplus energy when train operates in braking phase.

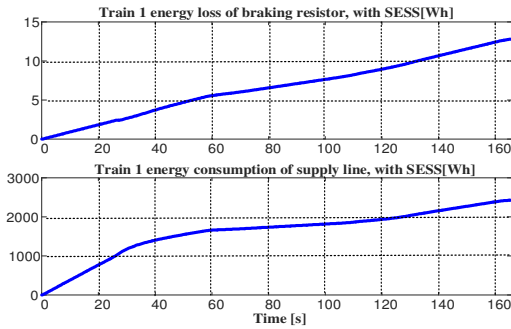


Figure 22. Dynamic behaviors of T1 energy, with SESS

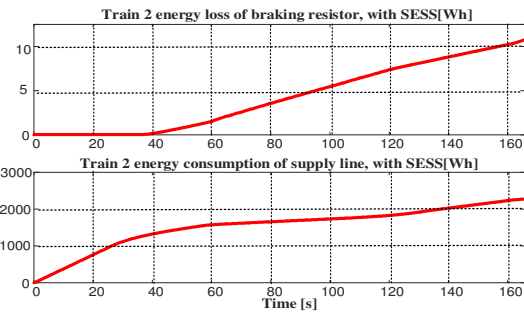


Figure 23. Dynamic behaviors of T2 energy, with SESS

Fig. 22,23 show dynamic responses of T1,T2 in energy loss on braking resistors and total consumption energy of supply line. The energy loss is little to compare with line energy, about 0.5%.

5. Conclusions

The use of SESS integrated with traction motor drive system, which is verified by simulation results for two electric trains operating in Metro line 2, Vietnam, with three different scenarios represents an effective solution for reducing voltage fluctuation of DC bus in accelerating, braking regimes of electrified train and the recovery of the kinetic energy during braking phase. These improvements can lead to a reduction of power demand allowing an increase of the distances between substations for new planned lines of Vietnam railway transportation in the coming time.

Acknowledgments

The authors would like to thank University of Transport and Communications for financial support, Institute for Control Engineering and Automation of HUST for creating a good research environment as well.

References

- [1] C. Xiao-li, Y. Jian and F. Yu, "Model and Simulation of a Super-capacitor Braking Energy Recovery System for Urban Railway Vehicles," *2010 WASE International Conference on Information Engineering*, Beidaihe, Hebei, 2010, pp. 295-300.
- [2] IEA and UIC, Railway handbook 2012 – energy consumption and CO2 emissions, International Energy Agency; 2012. <<http://www.uic.org/IMG/pdf/iea-uic>.
- [3] European Commission, Roadmap to a single European transport area- towards a competitive and resource efficient transport system; 2011.
- [4] A.Gonzalez-Gil,R.Palacin, P.Batty,J.P.Powell, "Energy-efficient urban rail systems: strategies for an optimal management of regenerative braking energy", *TRA-transport research arena 2014*, Paris.
- [5] González-Gil, A., Palacin, R., Batty, P., et al.: 'A systems approach to reduce urban rail energy consumption', *Energy Convers. Manag.*, 2014, 80, pp. 509–524.
- [6] Shuai Su *, Tao Tang and Yihui Wang, "Evaluation of Strategies to Reducing Traction Energy Consumption of Metro Systems Using an Optimal Train Control Simulation Model", *Energies*2016, 9, 105.
- [7] F. Du, J. H. He, L. Yu, M. X. Li, Z. Q. Bo and A. Klimek, "Modeling and Simulation of Metro DC Traction System with Different Motor Driven Trains," *2010 Asia-Pacific Power and Energy Engineering Conference*, Chengdu, 2010, pp. 1-4.

- [8] Kyoungmin Son, 1 Sejin Noh, 1 Kyoungmin Kwon, 1 Jaeho Choi, 2 Eun-Kyu Lee , Line Voltage Regulation of Urban Transit Systems Using Supercapacitors, 2009 IEEE 6th International Power Electronics and Motion Control Conference.
- [9] Kee-Hyun Chot), Su-Jin Jang, Byoung-Kuk Leel), Chung-Yuen Won, and Gil-Dong kim, Development of DC Line Voltage Simulatorfor Control of Regenerative Energy Storage Device in DC Traction System, The 7th International Conference on Power Electronics October 22-26, 2007 I Exeo, Daegu, Korea.
- [10] Kyoungmin Kwon, Eun-Kyu Lee, Jaeho Choi, Efficiency Improvement of ESS for DC Transit System, 2012 IEEE 7th International Power Electronics and Motion Control Conference - ECCE Asia June 2-5, 2012, Harbin, China.
- [11] Louis Romo, David Turner, L.S. Brian Ng, P.E, cutting traction power costs with wayside energy storage systems in rail transit systems, Proceedings of March 15 -18 2005 Joint Rail Conference Pueblo Colorado.
- [12] Bwo-RenKeKuo-Lung Lian Yu-Lung Ke* Tian-Hao Huang Muhammad Risky Mirwandhana , Control Strategies for Improving Energy Efficiency of Train Operation and Reducing DC Traction Peak Power in Mass Rapid Transit System, 6-11 May 2017 IEEE/IAS 53rd Industrial and Commercial Power Systems Technical Conference (I&CPS)
- [13] Kyoungmin Kwon, Kyoung-Gu Lee, Taesuk Kim, Jinkook Lee, Byoung-JeenJone, Jaeho Choi, IlhamiColak , Enhanced Operating Scheme of ESS for DC Transit System, 25-28 Sept. 2016 IEEE International Power Electronics and Motion Control Conference (PEMC)
- [14] Dr. Michael Steiner, Markus Klohr , Prof. Stanislaus Pagiela, Energy Storage System with UltraCaps on Board of Railway Vehicles, 2-5 Sept. 2007 European Conference on Power Electronics and Applications
- [15] Z. Gao, J. Fang, Y. Zhang, D. Sun, L. Jiang, and X. Yang, "Control Research of Supercapcitor Energy Storage System for Urban Rail Transit Network," *Inf. Sci. Electron. Electr. Eng. (ISEEE)*, 2014 *Int. Conf.*, pp. 181–185, 2014.
- [16] S. Noh, J. Choi, H. Kim, and E. Lee, "PSiM Based Electric Modeling of Supercapacitors for Line Voltage Regulation of Electric Train System," no. PECon 08, pp. 855–859, 2008.
- [17] K. Son, S. Noh, K. Kwon, J. Choi, and E. Lee, "Line Voltage Regulation of Urban Transit Systems Using Supercapacitors," vol. 3, pp. 933–938, 2009.
- [18] M. Khodaparastan and A. Mohamed, "Supercapacitors for electric rail transit systems," *2017 IEEE 6th International Conference on Renewable Energy Research and Applications (ICRERA)*, San Diego, CA, USA, 2017, pp. 896-901.
- [19] M. H. Akşit, S. Öztürk and I. Çadırcı, "A study on ultracapacitor-based systems for compensation of power deficiency and saving energy: Design, control and simulation," *2017 IEEE 3rd International Future Energy Electronics Conference and ECCE Asia (IFEEC 2017 - ECCE Asia)*, Kaohsiung, 2017, pp. 1008-1013.
- [20] F. Naseri, E. Farjah and T. Ghanbari, "An Efficient Regenerative Braking System Based on Battery/Supercapacitor for Electric, Hybrid, and Plug-In Hybrid Electric Vehicles With BLDC Motor," in *IEEE Transactions on Vehicular Technology*, vol. 66, no. 5, pp. 3724-3738, May 2017.
- [21] A. Capasso, R. Lamedica, A. Ruvio, M. Ceraolo and G. Lutzemberger, "Modelling and simulation of electric urban transportation systems with energy storage," *2016 IEEE 16th International Conference on Environment and Electrical Engineering (EEEIC)*, Florence, 2016, pp. 1-5.
- [22] M. H. Akşit, S. Öztürk and I. Çadırcı, "A study on ultracapacitor-based systems for compensation of power deficiency and saving energy: Design, control and simulation," *2017 IEEE 3rd International Future Energy Electronics Conference and ECCE Asia (IFEEC 2017 - ECCE Asia)*, Kaohsiung, 2017, pp. 1008-1013.
- [23] Z. Guiping, X. Mingchao and W. Siyu, "Hybrid power supply system of rail transit based on on-board energy storage equipment," *2014 International Conference on Power System Technology*, Chengdu, 2014, pp. 3124-3128.
- [24] C. Uyulan, M. Gokasan, and S. Bogosyan, "Modeling, simulation and slip control of a railway vehicle integrated with traction power supply," *Cogent Eng.*, vol. 17, no. 1, pp. 1–17, 2017.
- [25] C. S. Chang, A. Khambadkone, Z. Xu, and S. Member, "Modeling and Simulation of DC Transit System with VSI-fed Induction Motor Driven Train Using PSBIMIATLAB.," 4th IEEE international Conference on Power Electronics and Drive Systems- PEDS 2001 Indonesia.
- [26] M. Quraan and J. Siam, "Modeling and simulation of railway electric traction with vector control drive," *2016 IEEE International Conference on Intelligent Rail Transportation (ICIRT)*, Birmingham, 2016, pp. 105-110
- [27] Y. Zhang, Y. Gao, J. Li and M. Sumner, "Interleaved Switched-Capacitor Bidirectional DC-DC Converter with Wide Voltage-Gain Range for Energy Storage Systems," in *IEEE Transactions on Power Electronics*, 2017, vol. PP, no. 99, pp. 1-1.
- [28] Y. c. Zhang, L. l. Wu, X. j. Zhu and H. q. Liang, "Design of supercapacitor-based energy storage system for metro vehicles and its control rapid implementation," *2008 IEEE Vehicle Power and Propulsion Conference*, Harbin, 2008, pp. 1-4.

- [29] M. Islam, M. Nasrin and A. B. Sarkar, "An Isolated Bidirectional DC-DC Converter for Energy Storage Systems," *PCIM Europe 2017; International Exhibition and Conference for Power Electronics, Intelligent Motion, Renewable Energy and Energy Management*, Nuremberg, Germany, 2017, pp. 1-6.
- [30] C. Yoon, J. Kim and S. Choi, "Multiphase DC-DC Converters Using a Boost-Half-Bridge Cell for High-Voltage and High-Power Applications," in *IEEE Transactions on Power Electronics*, vol. 26, no. 2, pp. 381-388, Feb. 2011.
- [31] I. Azizi and H. Radjeai, "A bidirectional DC-DC converter fed DC motor for electric vehicle application," pp. 0-4, 2015.
- [32] Pham Tuan Anh, Vu Hoang Phuong, Nguyen PhungQuang, "Modeling and Control of Supercapacitor Energy Storage Systems", *Journal of Science and Technology Technical Universities*, No.103,2014.
- [33] S. Bacha, I. Munteanu, and A. I. Bratcu, *Power Electronic Converters Modeling and Control*, 2008.
- [34] Bimalk.bose, *Morden Power Electronics and AC Drives*, 2002.